Supporting Information

Allyl-terminated organic small molecule donors effectively regulate miscibility to improve the performance of organic solar cells

Jiaxin Dai [a], Panpan Zhang [a], Bo Du [a], MengYuan Ma[a], Shangrong Wu [a], Yuchuan Tian [c], Junyu Li [c]*, Haijun Bin [a, b]*, Yongfang Li [a, b]*

[a] Laboratory of Advanced Optoelectronic Materials, Suzhou Key Laboratory of Novel Semiconductor Materials and Devices, College of Chemistry, Chemical Engineering and Materials Science, Soochow University, Suzhou, 215123, Jiangsu, PR China.

E-mail: hjbin24@suda.edu.cn

[b] Jiangsu Key Laboratory of Advanced Negative Carbon Technologies, Soochow University, Suzhou, 215123, Jiangsu, PR China.

[c] Sinopec Shanghai Research Institute of Petrochemical Technology, Shanghai 201028, PR China.

Experimental Section

Instruments and Measurements

^{1}HNMR and MALDI-TOF-MS measurements

HNMR spectra were recorded in $CDCl_3$ on a Bruker AV 400 MHz FT-NM spectrometer, and chemical shifts are quoted relative to tetramethyl silane for ^{1}H. The molecular mass was confirmed by using an Ultraflextreme matrix-assisted laser desorption ionization mass spectrometer (MALDI-TOF-MS).

TGA and DSC measurements.

Thermogravimetric analysis (TGA) and differential scanning calorimetry (DSC) were conducted on METTLER-TOLEDO STARe at a heating rate of 10 ℃ min^{-1} and under an N_2 rate of 90 mL min^{-1}.

Electrochemical characterizations.

Cyclic voltammetry was performed on a Zahner IM6e electrochemical workstation with a three-electrode system in a 0.1 M $[Bu_4N]PF_6$ acetonitrile solution at a scan rate of 100 mV s^{-1}. A glassy carbon coated with a small-molecule film was used as the working electrode. A Pt wire was used as the counter electrode, and Ag/Ag^+ was used as the reference electrode. A ferrocene/ferrocenium redox couple was used as the external standard, and its redox potential was 0.11 V versus Ag/Ag^+. The HOMO and LUMO energy levels were calculated from the onset of the oxidation and reduction potential of the SMDs and acceptors using the following equations: E_{HOMO}/E_{LUMO}= -e ($\varphi_{ox}/\varphi_{red}$+4.8-$\varphi_{Fc}/\varphi_{Fc}^+$) (eV).

UV–vis–NIR absorption

Ultraviolet-visible-near infrared (UV–vis–NIR) absorption spectra was taken on an Agilent Technologies Cary 5000 Series UV–vis–NIR Spectrophotometer.

***J-V* and EQE measurements**

The current density-voltage (*J-V*) characteristics were recorded with a Keithley 2450. The power conversion efficiencies were measured under 1 sun, AM 1.5G (air mass 1.5 global) (100 mW cm^{-2}) using an SS-F5-3A (Enli Technology CO., Ltd.) solar simulator (AAA grade, 50mm × 50 mm photo-beam size). 2×2 cm^2 Monocrystalline silicon reference cell (SRC-00019, covered with a KG5 filter window) was purchased from Enli Technology CO., Ltd. The EQE was measured by Solar Cell Spectral Response Measurement System LST-QE (JinZhu Tech CO., Ltd.). The light intensity at each wavelength was calibrated with a standard single-crystal Si photovoltaic cell.

SCLC mobility measurements

The hole and electron mobilities of devices were evaluated from the space-charge-limited current (SCLC) method with the hole-only structure of ITO/PEDOT:PSS/blend films/MoO_3/Ag and electron-only structure of ITO/ZnO/blend films/PFN-Br/Ag, respectively. The corresponding charge mobilities were calculated from fitting the Mott-Gurney square law $J = 9\varepsilon_r\varepsilon_0\mu V_2/(8L^3)$, where J is the current density, ε_r is the dielectric permittivity of the active layer (assumed to be 3), ε_0 is the vacuum permittivity, L is the thickness of the active layer, μ is the hole or electron mobility. $V = V_{appl} - V_{bi} - V_s$, V_{appl} is the applied voltage, V_{bi} is the built-in voltage, V_s is the voltage drop from the substrate's series resistance (V_s =IR). The SCLC devices were measured under a dark condition in a nitrogen glovebox without encapsulation.

AFM measurements

The morphologies of the blend films were investigated by Atomic Force Microscope (AFM) measurements (Bruker, Multimode 8 SPM Systema) in contacting under normal air conditions at room temperature with 2 μm scanner.

TEM measurements

Transmission electron microscopy (TEM) was performed using a Tecnai G2 F20 S-TWIN instrument at 200 kV accelerating voltage, in which the blend films were prepared as following: First, the blend films were spin-coated on the PEDOT:PSS/ITO substrates; Second, the resulting blend film/PEDOT:PSS/ITO substrates were submerged in deionized water to make these blend films float onto the air-water interface; Finally, the floated blend films were taken up on unsupported 200 mesh copper grids for a TEM measurement.

TPC and TPV measurements

Transient photovoltage (TPV) and transient photocurrent (TPC) measurements were carried out under a 337 nm 3.5 ns pulse laser (160 μJ per pulse at 10 Hz) and halide lamps (150 W). Voltage and current dynamics were recorded on a digital oscilloscope (Tektronix MDO3102).

Contact angle measurements

The contact angle tests were performed on a Data physics OCA40 Micro surface contact angle analyzer. The surface energy was characterized and calculated by the contact angles of the two probe liquids (ultrapure water and diiodomethane).

GIWAXS measurements

GIWAXS measurements were carried out on the Xeuss 3.0 UHR system from Xenocs. The instrument is equipped with a Eiger 1M detector with a pixel size of 75um × 75um. The X-ray source is a Microfocus Sealed Tube X-ray Cu-source with the wavelength of λ = 1.54 Å. The sample was placed horizontally on the goniometer at a grazing angle of 0.2° relative to the incident beam.

Fabrication and Characterization of All-Small-Molecule Solar Cells

All the devices with a conventional device structure of ITO/PEDOT:PSS (30 nm)/active layers/PFN-Br (5 nm)/Ag (100 nm) were fabricated under conditions as follows. The patterned indium tin oxide (ITO) coated glasses were cleaned with detergent and then underwent a wet-cleaning process inside an ultrasonic bath procedure, followed by ultrapure water, acetone, and isopropanol in sequence, and then blown dry through high-purity nitrogen. After the treatment in a UV-Ozone Cleaner for

20 min, PEDOT:PSS (Heraeus Clevios PVP Al 4083) was deposited by spin-coating under 6000 rpm for 40 s on the cleaned ITO substrate. Then the films were annealed at a hot plate of 150 ℃ for 15 min in the air and the substrates were transferred into a glove box immediately.

The optimal H35:Y6 and H36:Y6 (2:1, w/w) are dissolved in chloroform (CF) with concentration of 20 mg mL^{-1}, which is placed to a hot plate at 60 ℃ for CF stirred for 12 h. The blend solution was spin-cast at 2000 ~ 2500 rpm for 40 s over the ITO glasses form a ~ 100 nm thickness of the active layer, followed by thermal annealing. H35:Y6 thermal annealing at 140 ℃ for 5 min, and H36:Y6 thermal annealing at 100 ℃ for 5 min.

The optimal H35:PY-IT and H36:PY-IT (2.7:1, w/w) are dissolved in chloroform (CF) with concentration of 16 mg mL^{-1}, which is placed to a hot plate at 60 ℃ stirred for 12 h. The blend solution was spin-cast at 2000 ~ 2500 rpm for 40 s over the ITO glasses form a ~ 100 nm thickness of the active layer, followed by thermal annealing at 140 ℃ for 5 min.

Next, the electron-transport material PFN-Br with a concentration of 0.5 mg mL^{-1} in methanol was spin-coated onto the active layer at 3000 rpm for 30 s. Finally, the Ag electrode (100 nm thickness) was vacuum-deposited onto the PFN-Br layer under a pressure of 4.0×10^{-4} Pa.

Detailed synthesis procedures

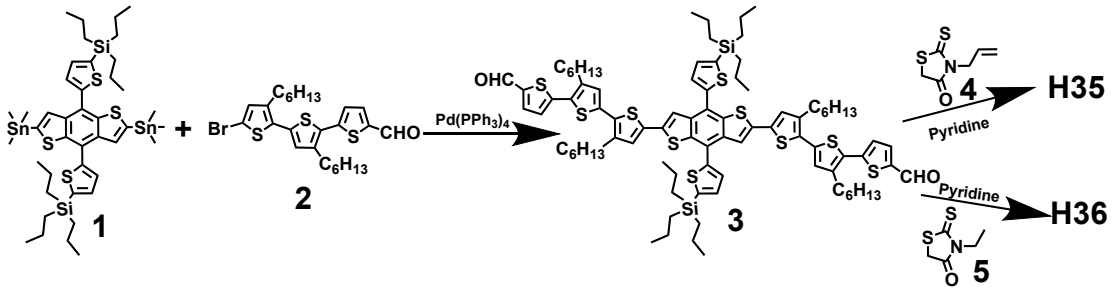

Synthesis of compound **3**：

Compound **1** (200 mg 0.201 mmol) and compound **2** (232.05 mg 0.44 mmol) were added into a 200 mL flask at room temperature, followed by dissolution in 20 mL of toluene. Subsequently, $Pd(PPh_3)_4$ (23 mg 10%) was added under argon protection. After the solution was stirred under reflux at 110 ℃ under the protection of argon for 24 h, the mixture was cooled to room temperature. The reaction was then quenched by addition of water. The mixture was extracted with CH_2Cl_2, and the combined organic layers were washed with brine, dried over dry Mg_2SO_4, and filtered. After removal of solvent, the crude product was purified by column chromatography on silica gel to afford compound **3** as a red solid (230 mg, 74.2% yield).

^{1}H NMR (400 MHz, $CDCl_3$) δ 9.88 (s, 2H), 7.71 (d, J = 4.0 Hz, 2H), 7.63 (s, 2H), 7.58 (d, J = 3.4 Hz, 2H), 7.40 (d, J = 3.4 Hz, 2H), 7.23 (d, J = 3.9 Hz, 2H), 7.11 (s, 2H), 7.01 (s, 2H), 2.83 – 2.75 (m, 8H), 1.71 – 1.66 (m, 8H), 1.46 – 1.29 (m, 31H), 1.25 (s, 5H), 1.06 (t, J = 7.2 Hz, 20H), 0.93 – 0.86 (m, 22H). MALDI-TOF MS: calcd. for $C_{86}H_{110}O_2S_{10}Si_2$, m/z = 1550.53; found 1551.064.

Synthesis of **H35**:

Compound **3** (200 mg, 0.128 mmol) and compound **4** (112 mg, 0.64 mmol) were dissolved in $CHCl_3$ (25 mL) under an argon atmosphere, and then piperidine (0.3 mL) was added into the mixture by syringe. The reaction was stirred at 65 °C for 6 h. Then,

the mixture was poured into water and extracted with CH_2Cl_2 for three times, the organic layer was dried over anhydrous Mg_2SO_4. After removal of solvent, the crude product was purified by silica gel using chloroform as eluent to afford the target material H35 as solid (180 mg, 75.5% yield).

^{1}H NMR (400 MHz, $CDCl_3$) δ 7.85 (s, 2H), 7.58 (d, *J* = 3.4 Hz, 4H), 7.40 (d, *J* = 3.4 Hz, 2H), 7.36 (d, *J* = 4.0 Hz, 2H), 7.20 (s, 2H), 7.10 (s, 2H), 7.00 (s, 2H), 5.87 (q, *J* = 5.5 Hz, 2H), 5.32 (s, 1H), 5.27 (t, *J* = 2.3 Hz, 2H), 5.24 (s, 1H), 4.74 (d, *J* = 5.8 Hz, 4H), 2.80 (d, *J* = 8.0 Hz, 8H), 1.69 (q, *J* = 7.6 Hz, 10H), 1.35 (dd, *J* = 7.1, 3.8 Hz, 16H), 1.26 (s, 15H), 1.08 (d, *J* = 7.2 Hz, 18H), 0.96 – 0.90 (m, 27H). MALDI-TOF MS: calcd. for $C_{98}H_{120}N_2O_2S_{14}Si_2$, m/z = 1861.50; found 1862.411.

Synthesis of **H36**:

The synthetic route of H36 is similar with that of H35, excepting for using compound **5** to replace compound **4**. The crude product was purified by silica gel using chloroform as eluent to afford the target material H36 as solid. (185 mg, 78.6% yield).

^{1}H NMR (400 MHz, $CDCl_3$) δ 7.82 (s, 2H), 7.58 (d, *J* = 4.6 Hz, 4H), 7.40 (d, *J* = 3.3 Hz, 2H), 7.33 (d, *J* = 4.1 Hz, 2H), 7.18 (d, *J* = 4.1 Hz, 2H), 7.07 (s, 2H), 6.98 (s, 2H), 4.17 (d, *J* = 7.2 Hz, 4H), 2.77 (dt, *J* = 17.0, 7.9 Hz, 8H), 1.68 (q, *J* = 7.5 Hz, 8H), 1.48 – 1.17 (m, 41H), 1.07 (t, *J* = 7.3 Hz, 19H), 0.99 – 0.87 (m, 24H). MALDI-TOF MS: calcd. for $C_{96}H_{120}N_2O_2S_{14}Si_2$, m/z = 1837.50; found 1837.395.

Supplementary Figures and Tables

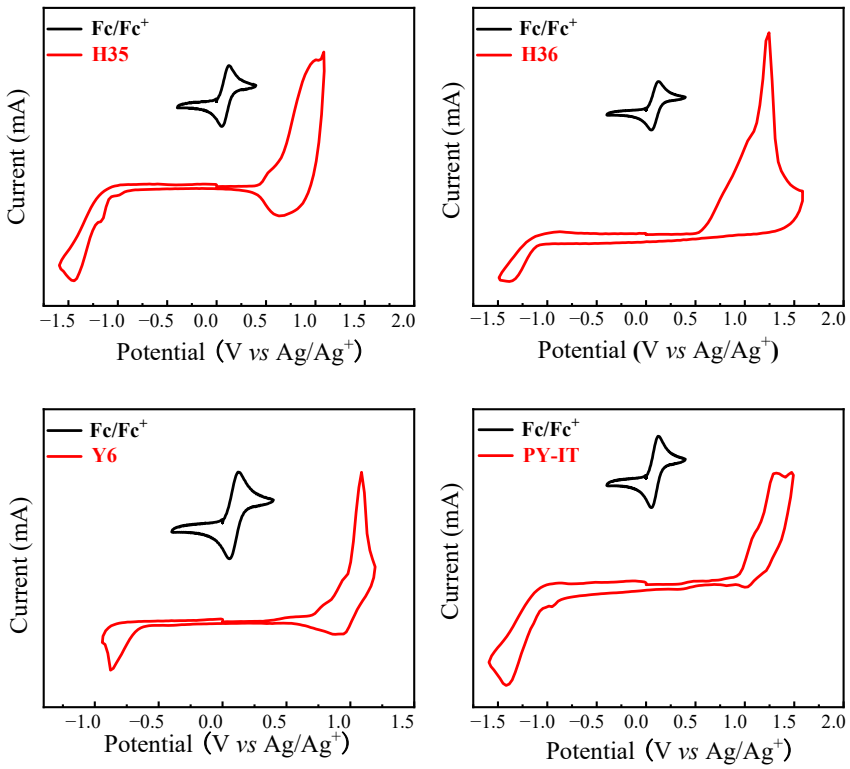

Figure. S1 CV curves of H35、H36、Y6 and PY-IT in the solid state, respectively. Ferrocene is used as the redox reference.

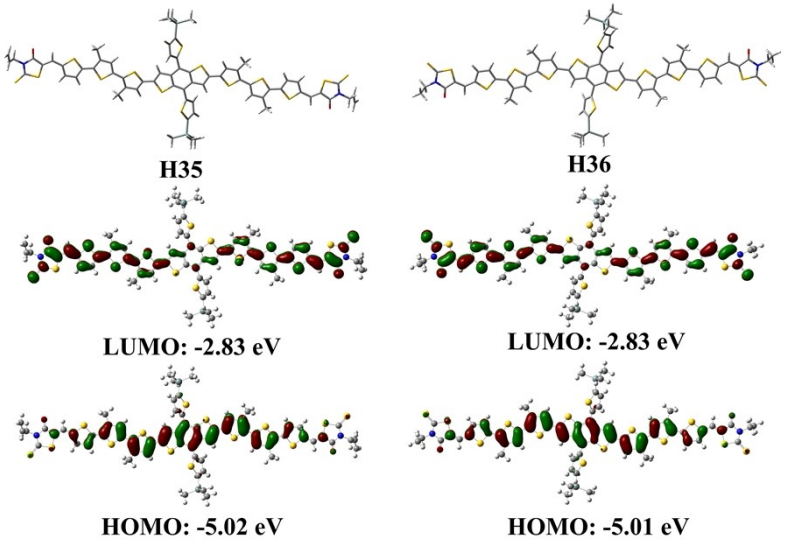

Figure. S2 The HOMO and LUMO energy levels of H35 and H36 derived from DFT simulations.

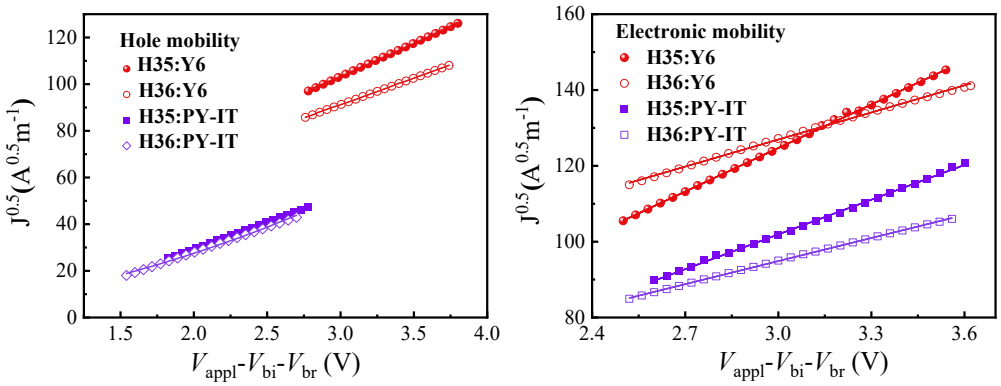

Figure. S3 Hole and electron mobilities for the blend films.

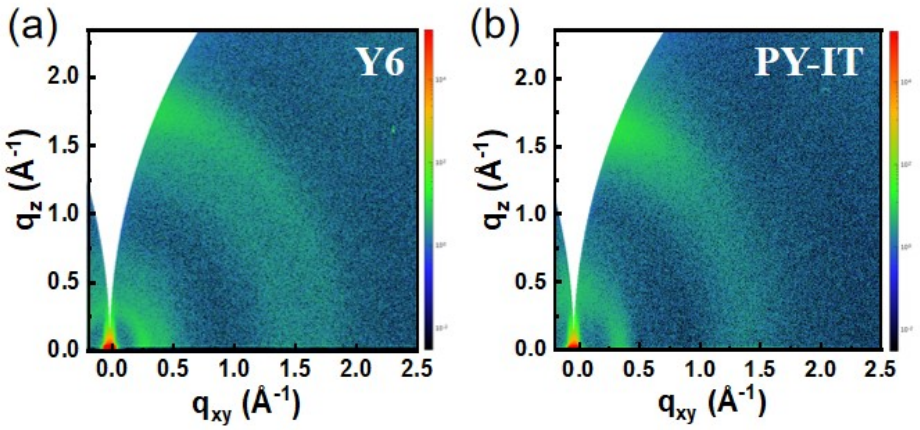

Figure. S4 2D GIWAXS diffraction patterns of (a) Y6 neat film; (b) PY-IT neat film.

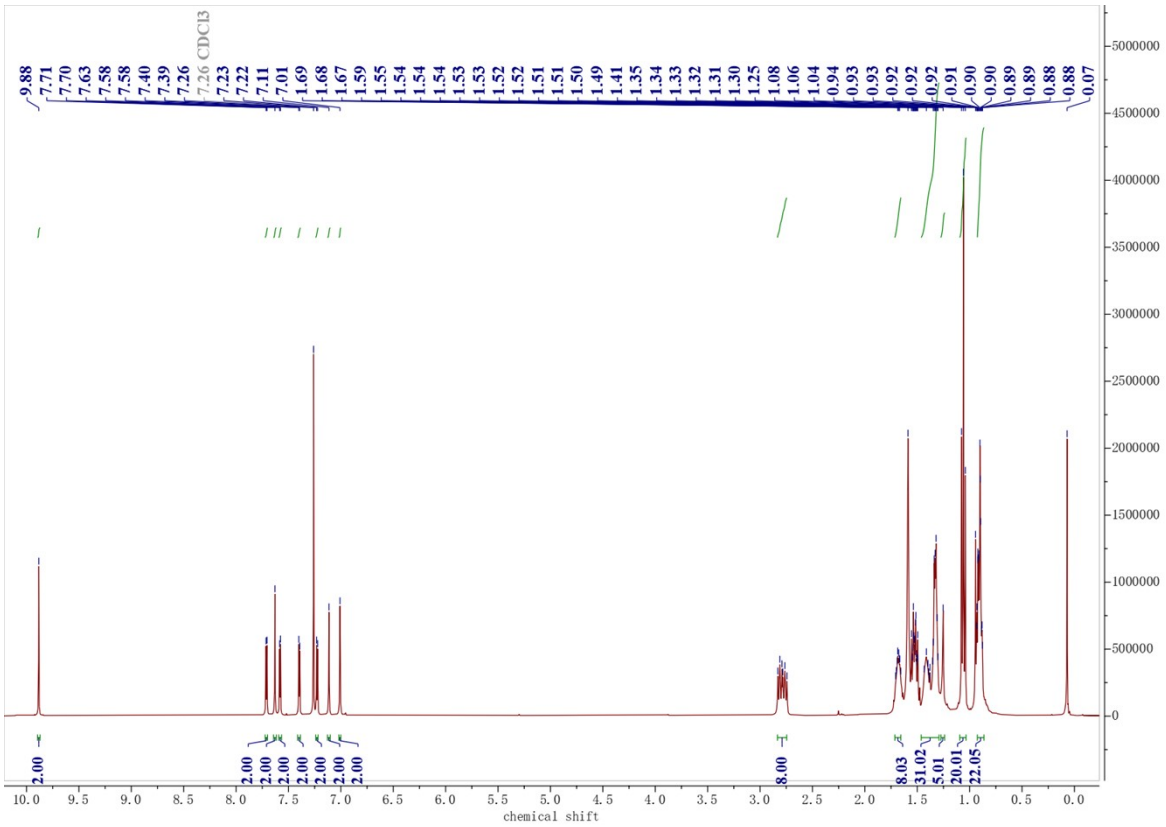

Figure S5. ^{1}H NMR spectra of compound **3** in $CDCl_3$.

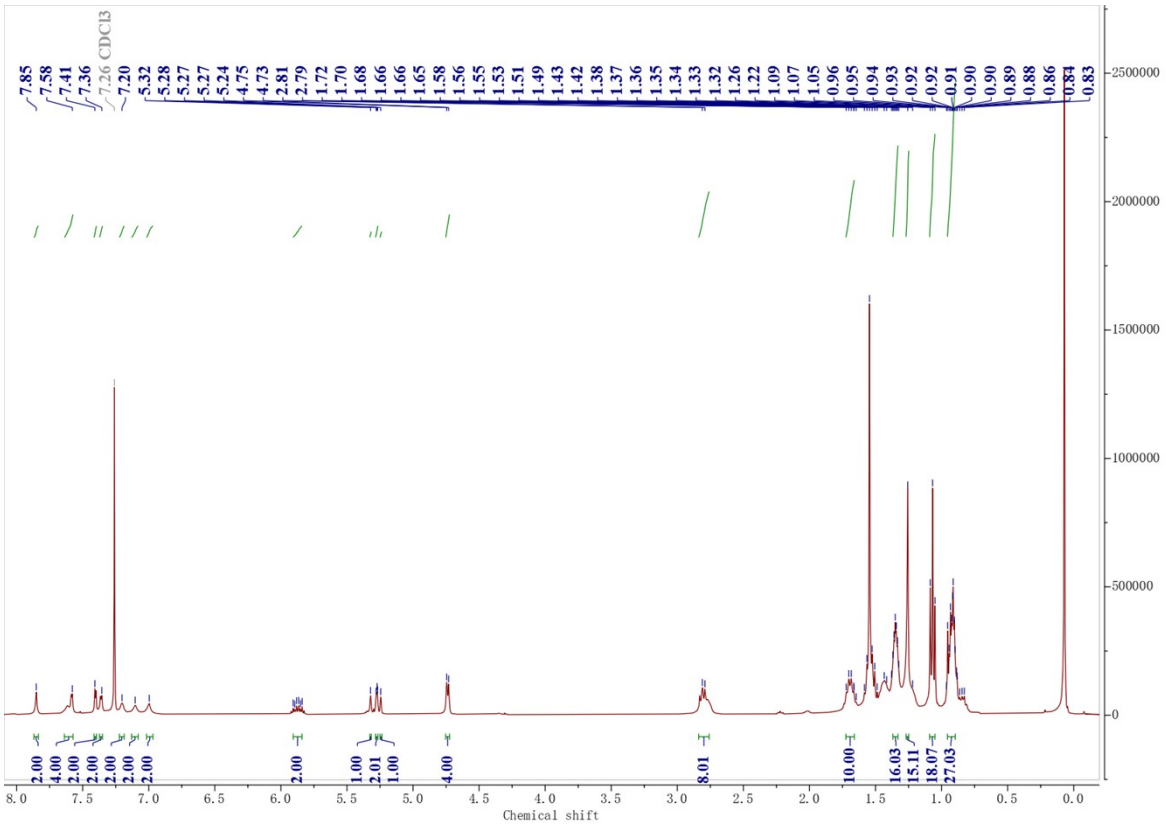

Figure S6. ^{1}H NMR spectra of **H35** in $CDCl_3$.

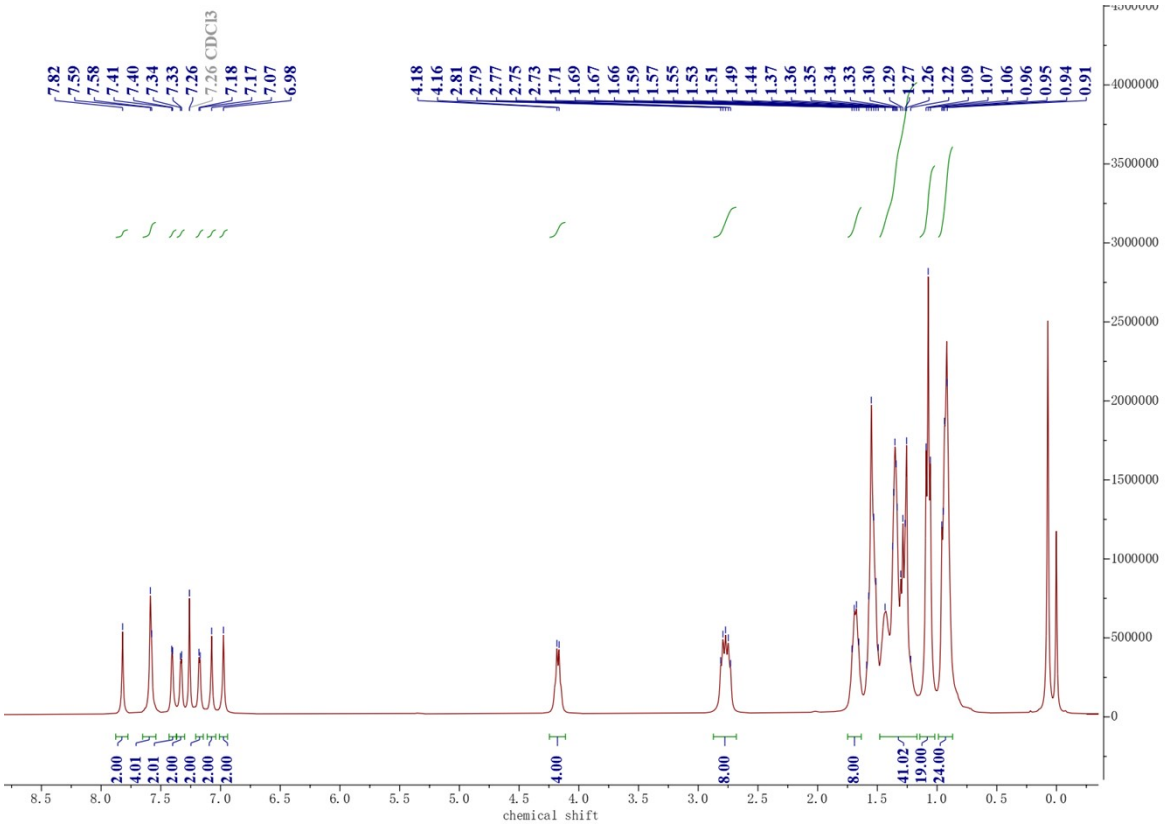

Figure S7. ^{1}H NMR spectra of **H36** in $CDCl_3$.

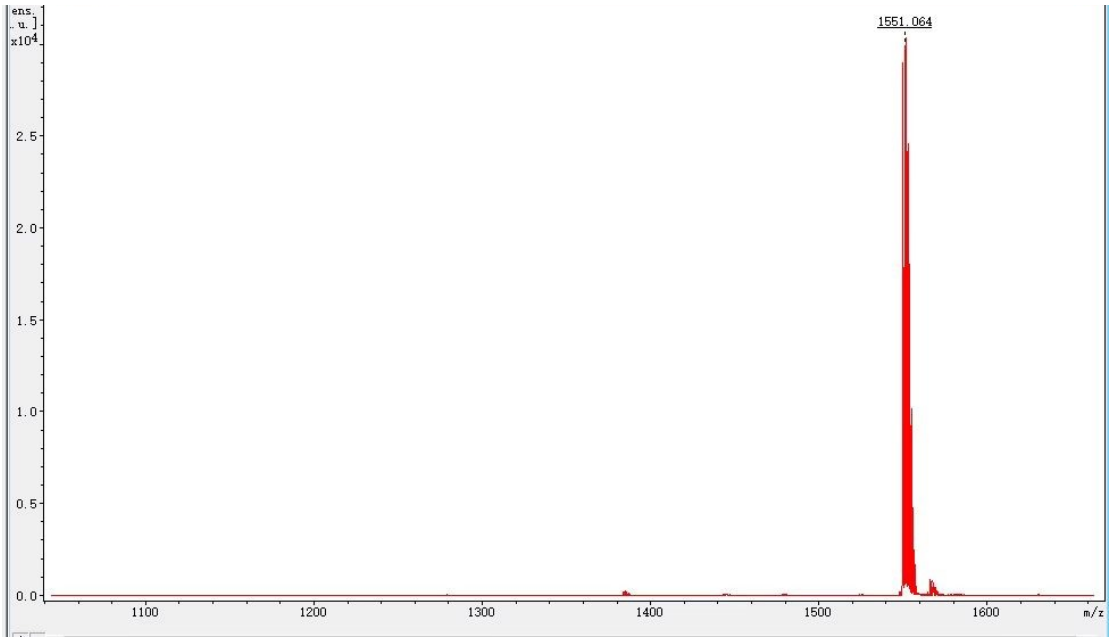

Figure S8. MALDI-TOF-MS spectra of compound **3**.

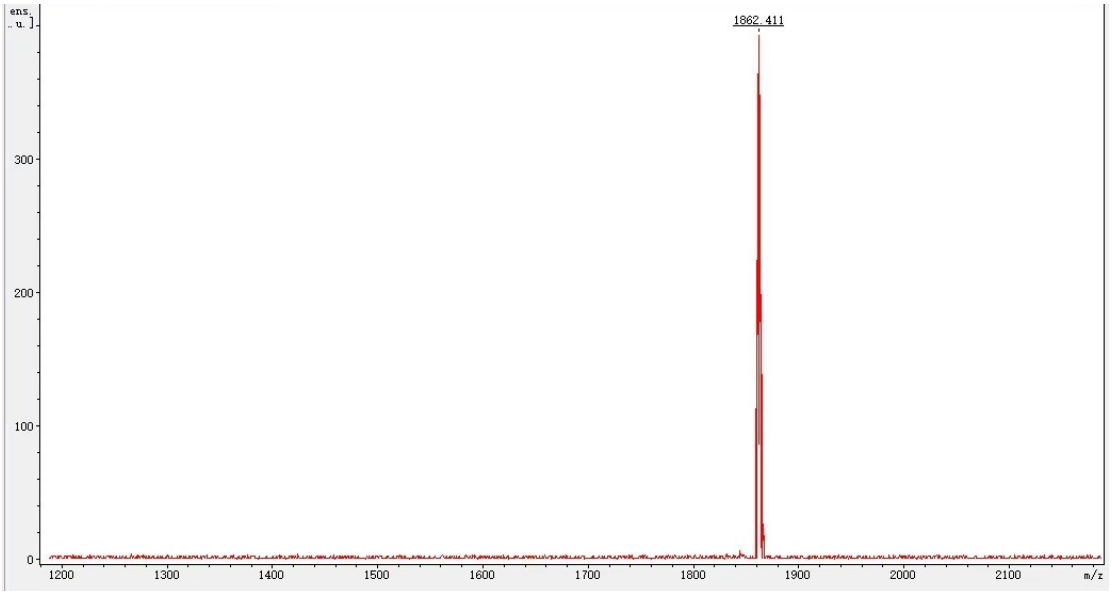

Figure S9. MALDI-TOF-MS spectra of **H35**.

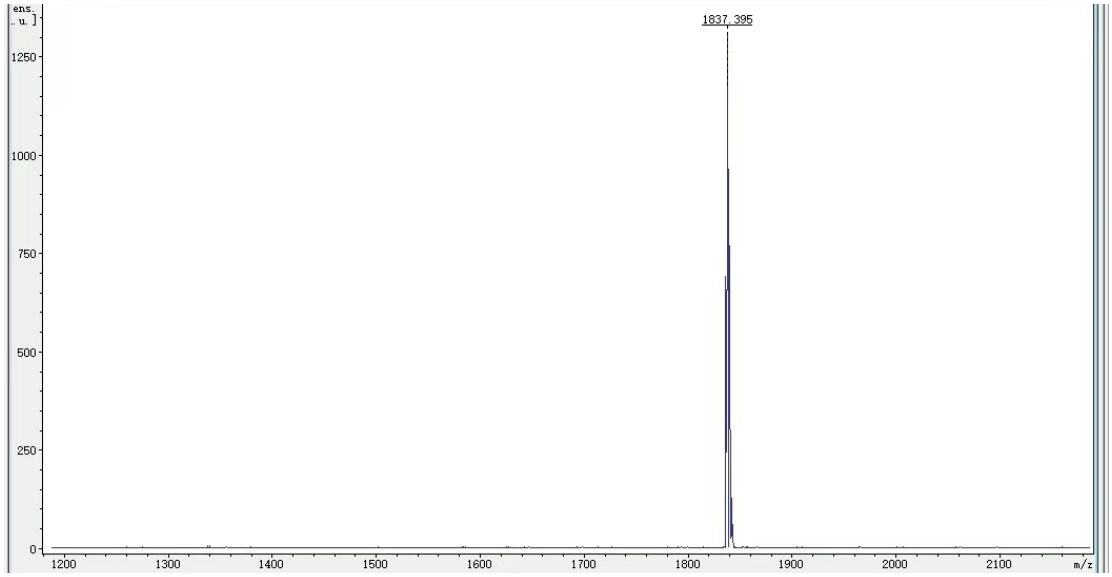

Figure S10. MALDI-TOF-MS spectra of **H36**.

Table S1. Optimization of H35:Y6-based ASM-OSCs. The parameters are obtained under the AM1.5G, 100 mW cm^{-2}.

Concentration	D:A	TA		V_{OC} (V)	J_{SC} (mA cm^{-2})	FF (%)	PCE (%)
20mg/ml	1.5:1	100℃	10min	0.866	21.66	46.30	8.68
20mg/ml	1.8:1	100℃	10min	0.858	21.90	50.25	9.44
20mg/ml	2.0:1	100℃	10min	0.855	22.17/21.88	51.29	9.72
20mg/ml	2.2:1	100℃	10min	0.854	20.20	45.94	7.93
20mg/ml	2.5:1	100℃	10min	0.849	18.95	45.15	7.26

20mg/ml	2.0:1	80℃ 5min	0.861	13.39	33.09	3.81
20mg/ml	2.0:1	100℃ 5min	0.865	19.61	45.03	7.64
20mg/ml	2.0:1	120℃ 5min	0.837	23.67	60.76	12.03
20mg/ml	2.0:1	140℃ 5min	0.784	25.16/23.95	69.46	13.70
20mg/ml	2.0:1	160℃ 5min	0.749	25.51	69.70	13.33
20mg/ml	2.0:1	140℃ 2min	0.787	25.03	67.93	13.38
20mg/ml	2.0:1	140℃ 5min	0.788	25.22	69.38	13.80
20mg/ml	2.0:1	140℃ 8min	0.788	25.98/24.45	68.06	13.93
20mg/ml	2.0:1	140℃ 10min	0.774	25.36	67.19	13.19
20mg/ml	2.0:1	140℃ 8min	0.821	26.34/25.10	70.39	15.21

Table S2. Optimization of H36:Y6-based ASM-OSCs. The parameters are obtained under the AM1.5G, 100 mW cm^{-2}.

Concentration	D:A	TA	V_{OC} (V)	J_{SC} (mAcm^{-2})	FF(%)	PCE (%)
20mg/ml	1.5:1	100℃ 5min	0.829	19.68	40.10	6.54
20mg/ml	2.0:1	100℃ 5min	0.846	20.07/19.45	49.22	8.35
20mg/ml	2.5:1	100℃ 5min	0.831	19.87	48.50	8.01
20mg/ml	3.0:1	100℃ 5min	0.668	18.76	32.52	4.07
20mg/ml	2.0:1	80℃ 5min	0.769	10.87	33.86	2.83
20mg/ml	2.0:1	100℃ 5min	0.844	19.62/19.48	50.56	8.37
20mg/ml	2.0:1	120℃ 5min	0.754	22.46	37.14	6.29
20mg/ml	2.0:1	140℃ 5min	0.330	21.71	29.63	2.12

Table S3. Optimization of H35:PY-IT-based SM:PA-OSCs. The parameters are obtained under the AM1.5G, 100 mW cm^{-2}. The optimized conditions were directly used to prepare H36:PY-IT devices.

Concentration	D:A	TA	V_{OC} (V)	J_{SC} (mA cm^{-2})	FF(%)	PCE (%)
16mg/ml	0.8:1	140℃ 10min	0.889	17.46	36.52	5.67
16mg/ml	1.0:1	140℃ 10min	0.905	19.96	42.13	7.61
16mg/ml	1.2:1	140℃ 10min	0.912	19.95	43.02	7.82
16mg/ml	1.4:1	140℃ 10min	0.918	20.68	43.18	8.20
16mg/ml	1.6:1	140℃ 10min	0.911	21.14	44.85	8.64
16mg/ml	1.8:1	140℃ 10min	0.912	20.84	46.12	8.77
16mg/ml	2.0:1	140℃ 10min	0.914	21.10	45.75	8.82
16mg/ml	2.2:1	140℃ 10min	0.924	20.00	50.45	9.32
16mg/ml	2.5:1	140℃ 10min	0.921	20.07	51.39	9.51
16mg/ml	2.7:1	140℃ 10min	0.919	20.38/19.46	53.15	9.96
16mg/ml	3.0:1	140℃ 10min	0.909	19.30	50.92	8.94

16mg/ml	2.7:1	120℃ 5min	0.945	18.41	50.02	8.71
16mg/ml	2.7:1	140℃ 5min	0.930	20.56/19.77	56.33	10.78
16mg/ml	2.7:1	160℃ 5min	0.914	20.71	56.69	10.73
16mg/ml	2.7:1	180℃ 5min	0.897	19.54	53.86	9.45
16mg/ml	2.7:1	200℃ 5min	0.846	18.16	53.50	8.23

Table S4. Hole and electron mobility of four devices under the optimized condition as those used for device fabrication.

Sample	μ_h (cm^2 V^{-1} s^{-1})	μ_e (cm^2 V^{-1} s^{-1})	μ_h/μ_e
H35:Y6	2.95×10^{-4}	2.75×10^{-4}	1.07
H35:PY-IT	2.03×10^{-4}	1.75×10^{-4}	1.16
H36:Y6	1.84×10^{-4}	1.37×10^{-4}	1.34
H36:PY-IT	1.45×10^{-4}	1.06×10^{-4}	1.37

Table S5. The detailed parameters of corresponding 1D GIWAXS profiles with (100) and (010) diffraction peaks for H35, H36, Y6 and PY-IT based neat films.

100	IP				OOP			
Sample	peak ($Å^{-1}$)	*d*-spacing (Å)	FWHM	CCL (Å)	peak ($Å^{-1}$)	*d*-spacing (Å)	FWHM	CCL (Å)
H35	0.32	19.63	0.068	92.35	0.34	18.47	0.056	112.14
H36	0.33	19.03	0.062	101.29	0.34	18.47	0.059	106.44
Y6	0.44	14.27	0.099	63.43	-	-	-	-
PY-IT	0.39	16.10	0.137	45.84	-	-	-	-

(010)	IP				OOP			
Sample	peak ($Å^{-1}$)	*d*-spacing (Å)	FWHM	CCL (Å)	peak ($Å^{-1}$)	*d*-spacing (Å)	FWHM	CCL (Å)
H35	1.72	3.65	0.201	31.24	1.70	3.69	0.115	54.61
H36	1.69	3.72	0.216	29.07	1.68	3.74	0.142	44.23
Y6	-	-	-	-	1.70	3.69	0.254	24.72
PY-IT	-	-	-	-	1.59	3.95	0.293	21.43

Table S7. The detailed parameters of corresponding 1D GIWAXS profiles with (100) and (010) diffraction peaks for H35, H36, Y6 and PY-IT-based blend films.

(100)	IP				OOP			
	peak ($Å^{-1}$)	*d*-spacing (Å)	FWHM	CCL (Å)	peak ($Å^{-1}$)	*d*-spacing (Å)	FWHM	CCL (Å)

H35:Y6	0.32	19.63	0.065	96.62	0.33	19.03	0.063	99.68
H36:Y6	0.33	19.03	0.064	98.13	0.34	18.47	0.066	95.15
H*35*:PY-IT	0.31	20.26	0.066	95.15	0.33	19.03	0.056	112.14
H36:PY-IT	0.33	19.03	0.073	86.03	0.35	17.94	0.064	98.13

(010)	IP				OOP			
	peak ($Å^{-1}$)	*d*-spacing (Å)	FWHM	CCL (Å)	peak ($Å^{-1}$)	*d*-spacing (Å)	FWHM	CCL (Å)
H35:Y6	-	-	-	-	1.71	3.67	0.172	36.51
H36:Y6	-	-	-	-	1.70	3.69	0.192	32.71
H*35*:PY-IT	-	-	-	-	1.69	3.72	0.201	31.24
H36:PY-IT	-	-	-	-	1.65	3.80	0.229	27.42

Table S8. Summary of contact angles (θ), surface tensions (γ) and Flory-Huggins interaction parameters (χ) for H35, H36, Y6 and PY-IT films.

Sample	θ_{water} (°)	θ_{DIM} (°)	γ (mN m^{-1})	$\chi_{D\text{-}A}$
H35	104.5	41.5	41.98	-
H36	100.5	37.5	43.15	-
Y6	88.5	39.0	40.14	-
PY-IT	91.5	40.0	39.82	-
H35:Y6	-	-	-	0.020κ
H36:Y6	-	-	-	0.054κ
H35:PY-IT	-	-	-	0.029κ
H36:PY-IT	-	-	-	0.067κ

The Flory-Huggins interaction parameter between the donor and acceptor is calculated through the equation: $\chi = k(\sqrt{\gamma_A}-\sqrt{\gamma_D})^2$